FINAL REPORT

for

NASA Contract NAS 8-32127

(Control No. 1-6-EC-06923(IF))

STUDY OF STRAY LIGHT SUPPRESSION FOR THE LARGE SPACE TELESCOPE

B. B. Fannin

Optical Sciences Center
University of Arizona
Tucson, Arizona 85721

March 5, 1980

FINAL REPORT

Contract NAS 8-32127

STUDY OF STRAY LIGHT SUPPRESSION FOR THE LARGE SPACE TELESCOPE

This report was prepared by the Optical Sciences Center of the University of Arizona under Contract NAS 8-32127, Study of Stray Light Suppression for the Large Space Telescope, for the George C. Marshall Space Flight Center of the National Aeronautics and Space Administration. This report, together with a 9" magnetic computer tape and the computer listing (268 pages) of the latest version of APART-6, completes the requirements for deliverable items under the contract.

CONTRACT HISTORY

Work to analyze stray radiation problems in large optical systems was first authorized by NASA Contract NAS 8-27804 (Stray Light Suppression Study for the Large Space Telescope) which was issued by MSFC to the Optical Sciences Center of the University of Arizona with an effective starting date of November 15, 1971. This contract was extended several times and was finally terminated on September 3, 1975, with the delivery of a computer program (APART-1, Analysis Program, Arizona's Radiation Trace) and copies of the User's Manual.

Contract NAS 8-32127 was issued by MSFC to the U of A to provide for further work on stray radiation analysis from the period from August 17, 1976 through August 16, 1977. By the end of the contract period the contract funds were essentially depleated and NASA did not contemplate a contract extention due to a lack of available funding. However, in return for certain services performed by NASA, the University of Arizona agreed to continue stray light suppression studies as an internally funded effort, and a one-year no-cost extention of Contract NAS 8-32127 was issued by MSFC on August 17, 1977.

On February 24, 1978, Mr. Robert Breault of the University of Arizona visted MSFC and presented a technical briefing on inprovements and increased capabilities of the APART program. At this time he delivered a magnetic tape copy of the APART-5 program, together with the latest User's Manual. APART-5 had numerous improvements over the original APART-1.

Although Contract NAS 8-32127 had a nominal expiration date of August 16, 1977, the APART-6 program delivered as part of this final report contains all improvements made to the original APART through September, 1979.

PROGRAM IMPROVEMENTS

Efforts to simplify and increase the efficiency of the program have continued and computer run times required for a typical analysis have been reduced to about 1/5th of the time required by the original program. Offsetting this economy, of course, is the ability of the program to handle the analysis of more complex systems, for which run times may increase. It is not a trivial matter (considering either personnel effort or computer time) to perform an accurate scattered light analysis of a complex optical system.

The original APART was developed to analyze an essentially rotationally-symmetric system (the LST). APART can now handle a large number of non-rotationally symmetric systems, such as systems with square or rectangular apertures and/or optical elements, systems with struts, and off-axis systems such as Z-systems. Some work has been done on incorporating transmissive optics, and some preliminary consideration has been given to incorporating diffraction effects; however, APART-6 does not have extended diffraction analysis capability. The program has also added limited capability for handling specular reflections.

PROGRAM DESCRIPTION

Other stray light analysis programs (GUERAP I, II, and "II) use either Monte Carlo or randomally selected ray-trace techniques to determine how much unwanted stray light entering the entrance aperture reaches the image plane. Although reasonably accurate, these programs require a great deal of computer time and give little information as to the critical paths by which the stray light reaches the image plane, making it difficult to improve the design of a system which does not meet performance requirements.

APART uses a different technique; the analysis starts at the image plane and progresses from there through the optical system to the front end of the telescope tube. The evaluation utilizes the y, $\overline{y}$ diagram, a powerful geometrical tool which enhances appreciation of all the first-

order or paraxial properties of the optical system. Only objects (or surfaces) which are "seen" by the image plane can contribute scattered light to the image plane; these objects are quickly identified and are eliminated from the "field of view" if possible. If they cannot be eliminated, effort is expended to insure that unwanted energy does not reach these surfaces. This approach identifies all areas which create scattered light problems in the system and often permits dramatic improvements to the system with a minimum of effort. If troublesome areas cannot be "eliminated", special surface coatings, etc., can be applied to these areas in order to reduce scattered light. APART is so structured that repeated analysis runs may be made on a system at a fraction of the cost of the original complete analysis.

APART consists of three main programs:

Program One makes the y, $\bar{y}$ analysis of the system and identifies all critical surfaces. Many times an analysis of the computer print-out of the optical system as analyzed by Program One will reveal serious design defficiencies which should be corrected before any more extensive analysis is made. Program One can now handle non-rotationally symmetrical systems, off-axis systems, etc.

Program Two computes the Geometrical Configuration Factors (GCF) from each area of the system under study to all other areas of the system. In general, large areas are broken down into a number of smaller areas--more areas for more accurate analysis, etc. This program not only determines the subtended area of each object as viewed by another object, but determines incident and reflected angles (these are important for baffle surfaces which do not have Lambertian scattering characteristics). Program Two can now handle struts as obscurations, off-axis or tilted detectors, tilted and decentered real space objects, sliced cones, eliptical obscurations, and toroidal obscurations.

Program Three computes the power input into the optical system (from either point source objects or extended objects such as the bright earth). Then the GCF values from Program Two and surface scattering characteristics are combined so that power transfers to the image plane are computed. Point Source Transmittance (PST) or Attenuation Factors are calculated for any desired off-axis angles for unwanted sources, and are plotted by the computer program.

MAGNETIC TAPE FORMAT

APART is supplied to MSFC recorded on a computer-compatable magnetic tape. The format of the program on the tape is:

9-Track tape
800 BPI
Odd Parity
3 Files (One for each of the three main APART subprograms)
80 Character records
40 Records/Block

In addition, a computer print-out of the program listing was supplied; this is in the form of 268 pages of 8-1/2 X 15 inch computer paper.

LIGHT SCATTERING FROM SURFACES IN OPTICAL SYSTEMS

When a source of unwanted radiation enters the aperture of an optical system, the energy impinges on various surfaces within the system; from these surfaces the energy is scattered and re-scattered until some fraction of the total input energy reaches the image plane as an unwanted interference signal. There are six general types of scattering mechanisms which enter into this propagation of unwanted energy through the system:

1. Baffle Surfaces--Baffle surfaces are intended to absorb as much of the incident radiation as possible; some fraction, however, is scattered, usually roughly into a hemisphere. These surfaces are known as "black", or diffuse, surfaces; depending on the wavelength, etc., a "good" diffuse surface will have approximately 1% total hemispherical scattering. Poorer surfaces will have 10% or more scattering.

2. Specular Reflectance from Black Surfaces.--Some "black" surfaces do not have ideal (Lambertian) diffuse scattering, but may have a specular reflectance which is quite high--10% or more of the incident energy. If this specular reflectance is directed to a harmless location, it may do little damage, but if the specular beam directly reaches the image plane it can create havoc.

3. Scattering from Mirror Surfaces--An ideal mirror surface directs all of the incident energy in an infinitely narrow beam along the angle of reflection. Any unwanted energy hitting such a surface is coming from a source angle outside the "field of view", so the

reflected beam will not hit the image plane. However, all mirror surfaces have some percentage of the incident energy scattered at angles other than the reflectance angle; this scattered energy may directly reach the image plane. The scattering properties of specular surfaces are usually expressed in the form of BRDF (Bidirectional Reflectance Distribution Function), which is a measure of the fraction of the incident light which is scattered into a specified solid viewing angle. This scattering is a strong function of incident angle, viewing angle, smoothness and cleanliness of the surface, and wavelength. A very good specular surface will have a BRDF of 10^{-5}/sr or less, poor surfaces may be as high as 10^{-2}/sr or more.

4. Diffraction--When an electromagnetic wave passes around the edge of a surface, the demarkation line near the edge is not well defined. Energy which hits the surface squarely is blocked by the surface (though some of the energy is reflected or scattered); energy which misses the edge continues unaffected. However, energy which "grazes" the edge is diffracted according to the well known laws of diffraction. This diffracted energy may reach the image plane as a serious source of stray radiation.

5. Internal Scattering from Transmissive Optics--Transmissive optics (lenses, etc.) all have some internal scattering due to imperfections in the material. If the energy passing through the lens is "wanted" energy, i.e., from an object in the field of view, this scattering will create some haze around the image. If the energy is from an unwanted source (outside the field of view), the scattered energy may reach the image plane, causing interference.

6. Internal Thermal Emission--This effect is not a scattering source, but may affect the signal-to-noise ratio at the image plane. Objects inside an optical system which are at a higher temperature than the image plane will radiate thermal energy which may reach the image plane. If this energy is within the acceptance wavelength of the detector, it will appear as noise.

An ideal scattered light analysis program will handle all six types of scattering listed above. APART-6 has very limited capability in handling four types--diffraction, specular reflectance of "black" surfaces, transmissive scattering, and internal thermal

radiation. However, for most optical systems (including the LST), the diffuse scatter from baffle surfaces and the near-specular scatter from polished surfaces are the predominant sources of unwanted scattering; APART-6 handles these two types of scattering with great dispatch and accuracy.

Systems which operate in the long-wave length portion of the optical spectrum (IR systems from 10 um to 300 μm) may have dominant scattering contributions from diffraction and/or internal thermal radiation, and APART-6 must be applied with care. Likewise, systems with a number of transmissive elements may require special handling.

It is seen that an accurate knowledge of the scattering characteristics of both mirror and "black" surfaces is required in order to perform an accurate scattered light analysis of an optical system. For the past 8-10 years, the Optical Sciences Center has been active in the determination of the scattering properties of both baffle and mirror surfaces. This work has been performed under a number of contracts, including NAS 8- 27804 and NAS 8-32127. The most important of the other contracts were Contract DAAG46-75-C-0085 for the Army Material and Mechanics Research Center [1] and DAAH01-75-C-0912 for the MICOM group at Red Stone Arsenal in Huntsville, Alabama.

Many organizations have made investigations into the scattering properties of baffles and polished surfaces at visible wavelengths. The results of these investigations are well documented in a number or articles.[2]

For the past several years, OSC has concentrated on investigating surface scattering properties in the Infrared (especially at 10.6 μm), an area which has been largely ignored in the past. This report will include some of the findings which were made during these investigations; some of the material has been previously published, but much has not.

[1] See Final Report, Contract Number DAAG46-75-C-0085, AMMRC Ctr 76-42, "A Study Leading to Improvements in Radiation Focusing and Control in Infrared Sensors", W. Wolfe, B. Fannin, et al, Dec. 1976

[2] See "Literature Survey for Suppression of Scattered Light in Large Space Telescopes", W. Tifft and B. Fannin, Feb. 1973, Univ. of AZ under Contract NAS 8-27804.

SCATTERING MEASUREMENTS

Figure 1 is a simplified block diagram of the set up used for making scattering measurements. The sample under test is illuminated by a light source (laser) of the desired wavelength; the light beam is chopped with a mechanical chopper so that a lock-in amplifier may be used for signal detection to greatly reduce background noise. A detector picks up the light scattered at the angle selected.

A more complete representation of the instrument used for this measurement program is shown in Figure 2; it is called BRDFRI (BRDF Recording Instrument). This machine was designed for rapid, accurate data acquisition. There are four degrees of freedom for the instrument: (1) detector arm angle, (2) sample incident angle, (3) sample tilt angle, and (4) laser polarization angle. The geometry of BRDFRI is based on the idea that the incident and reflected rays intersect at the sample, so these two lines define a plane of incidence; this plane can always be kept horizontal. This geometry was chosen such that the sample holder is the only component which needs to be rotated about other than a vertical axis, even when making measurements outside the plane of incidence. This feature facilitates the use of liquid-cooled detectors and interchangeable lasers.

The BRDF is a function of four angular variables, the elevation and azimuth of both the incident and reflected rays as measured from the surface of the sample. Only cuts out of the plane of incidence require changing more than the detector angle for a given incidence angle. Consequently, manual operation can be performed without difficulty for the normal mode of operation (measurements made in the plane of incidence). Scans made out of the plane of incidence are more time consuming.

Two important features (laser polarization and speckle averaging) have been incorporated into BRDFRI. The CO_2 laser (10.6 μm) has a wire grid polarizer in the cavity which provides a high degree of plane polarization; the laser may be mechanically rotated about the axis of the tube, providing polarization selection capability. Speckle averaging is accomplished by rapid sample rotation about its Z-axis.

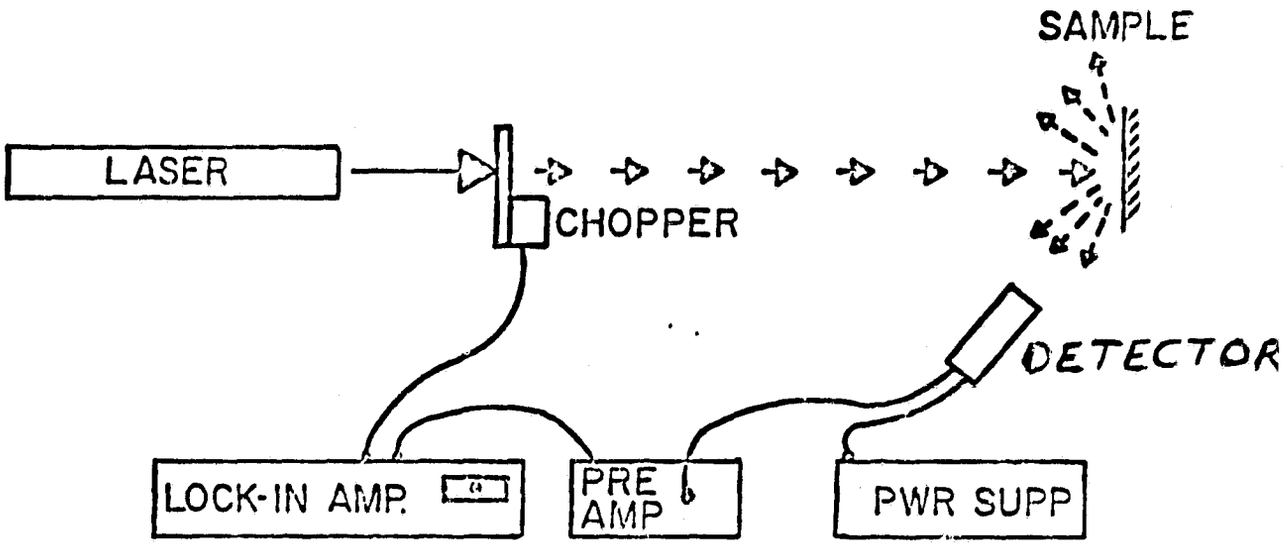

Figure 1: Schematic Diagram of Scatter Measurement Apparatus.

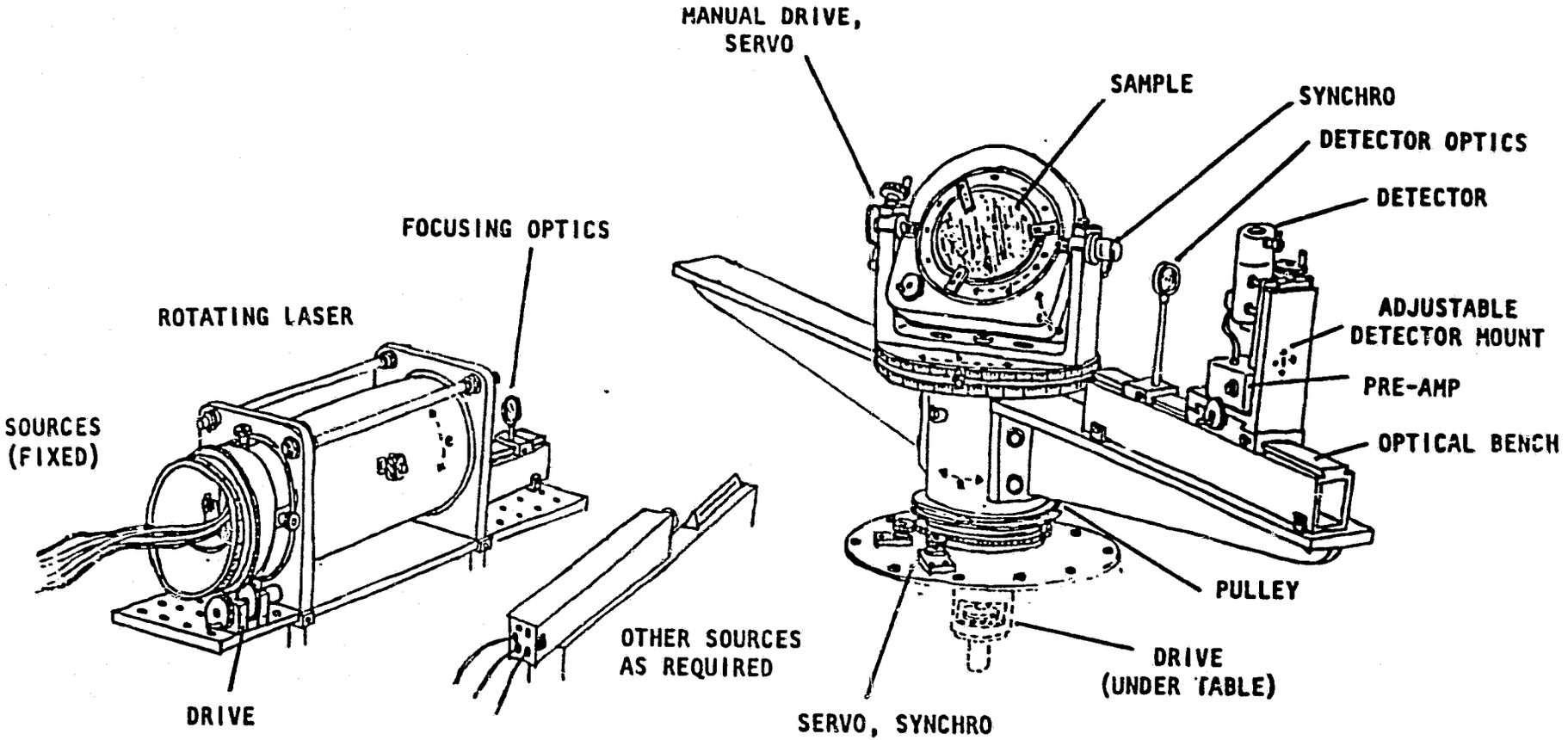

BRDF RECORDING INSTRUMENT (BRDFRI)

Figure 2

Form of Data Presentation

The results of the BRDF scattering measurements are plotted on log-log paper. The ordinate is BRDF, in units of reciprocal steradian. BRDF is defined as the ratio of the radiance at the detector divided by the irradiance on the sample; using the constant radiance properties of a Lambertian surface, the equation becomes

$$\text{BRDF} = \frac{V_S \rho_D}{V_D \gamma \pi}, \qquad \text{where}$$

V_S is the detector signal voltage with the sample of interest in place; V_D is the detector signal voltage with a reference sample in place; ρ_D is the total reflectivity of the diffuse reference; and γ is the cosine of the angle between the surface normal and the detector.

Thus, a 100% reflecting sample with a Lambertian (perfectly diffuse) reflectance would appear graphically as a straight line at the $1/\pi$ level (the integral of this over a hemisphere is equal to 1.0).

The abscissa of the graph is the angle of the detector with respect to the specular beam, in terms of $\beta - \beta_o$. The β's refer to the direction cosine space, which has the property that (for specular surfaces) the graphs of a surface at different angles of incidence lie on top of each other, i.e., the scattering function is shift invariant. To convert from direction cosines to actual angles, use the relationship $\theta = \sin^{-1}\beta$ and $\theta_o = \sin^{-1}\beta_o$. The range of this unitless abscissa is from 0 to 2. A range of 2 corresponds to seeing the backscatter edge-on while illuminating the surface at grazing angle.

Two items warrant explanation to advoid confusion in using the graphs. First, as a consequence of plotting the data using direction cosines, the curves for larger angles of incidence are shifted to the left for the same angle from the specular beam. Secondly, data on the left half of the graph corresponds to small angles from the specular beam (in most cases less than 10^o), and this half is emphasized due to plotting the data on log-log paper. It should be noted that log-log plots for specular surfaces yield straight lines, the slope of which is of importance to users of the data.

BRDF of "Black" Baffle Materials

Figure 3 shows the BRDF characteristics of some diffuse "reference" samples. NaCl (powdered) is a little flater than the gold-plated sandpaper, but its total integrated hemispherical reflectance is only about 93%, compared with 97% for the sandpaper. Also, NaCl is not very durable, so the 80-grit gold-plated sand paper was chosen as the "Standard" for further measurements.

Figure 4 shows the BRDF characteristics of nine different baffle coating materials which were tested. All of them are diffuse except #10, Cat-a-lac Black paint, which is a specular black. The turn-up for #7, 3M Nextel Black Velvet, at larger angles is normal for that material; it is due more to the $\cos^{-1}$ factor than to an increase in signal.

Figure 5 is similar to figure 4, with some of the same samples; however, samples #1, 4, 7, & 8 are new materials.

Martin Black Anodize was found to be the coating material with the lowest BRDF under most conditions, although this is not evident in figures 4 & 5. The Martin samples for those tests were not of high quality. Figure 6 shows the test results on a new Martin Black sample at various angles of incidence. Note that this diffuse material is not shift invarient (the curves change position with changes in the angle of incidence).

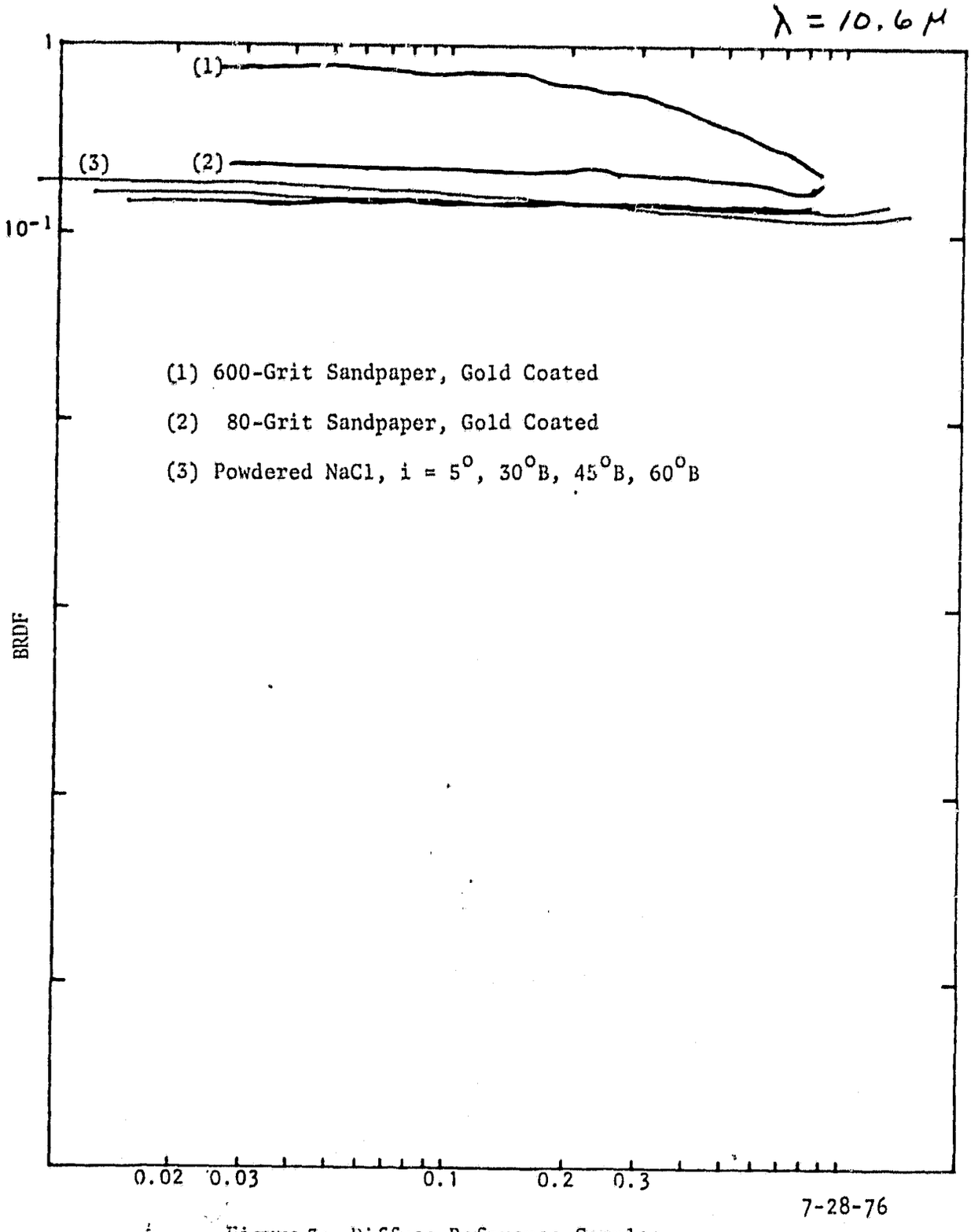

Figure 3: Diffuse Reference Samples

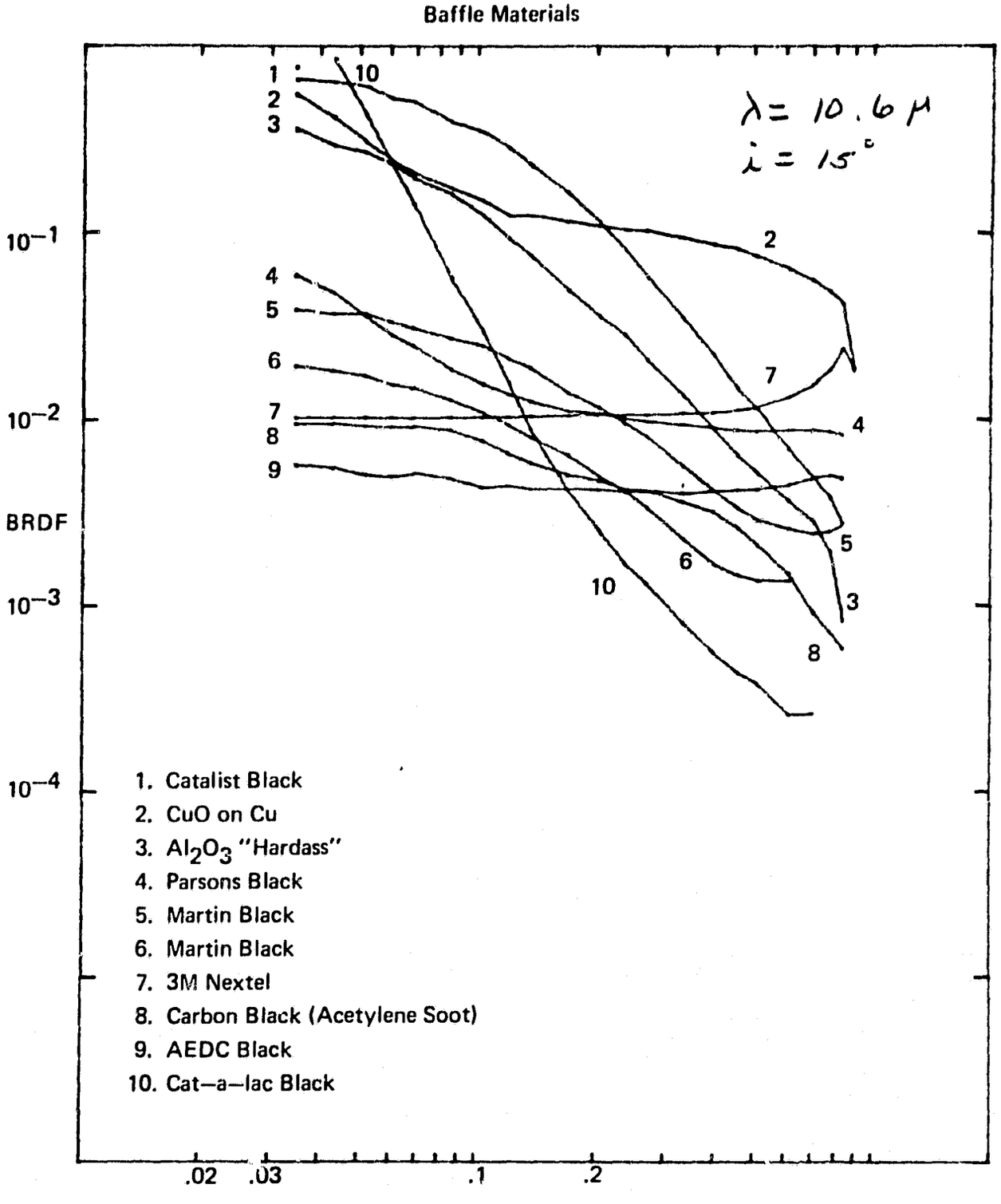

Figure 4 : Various Baffle Coating Materials

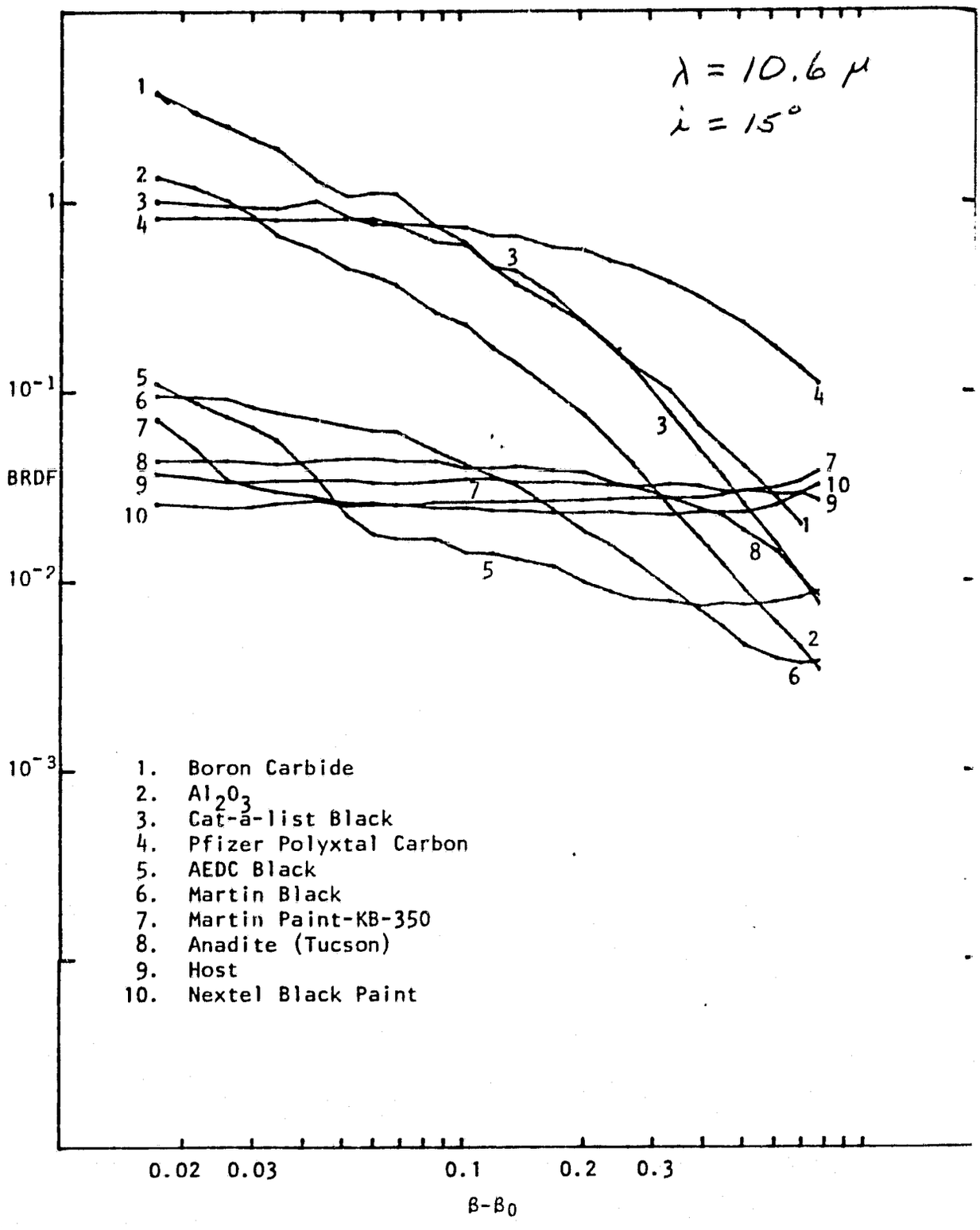

Figure 5: Baffle Materials

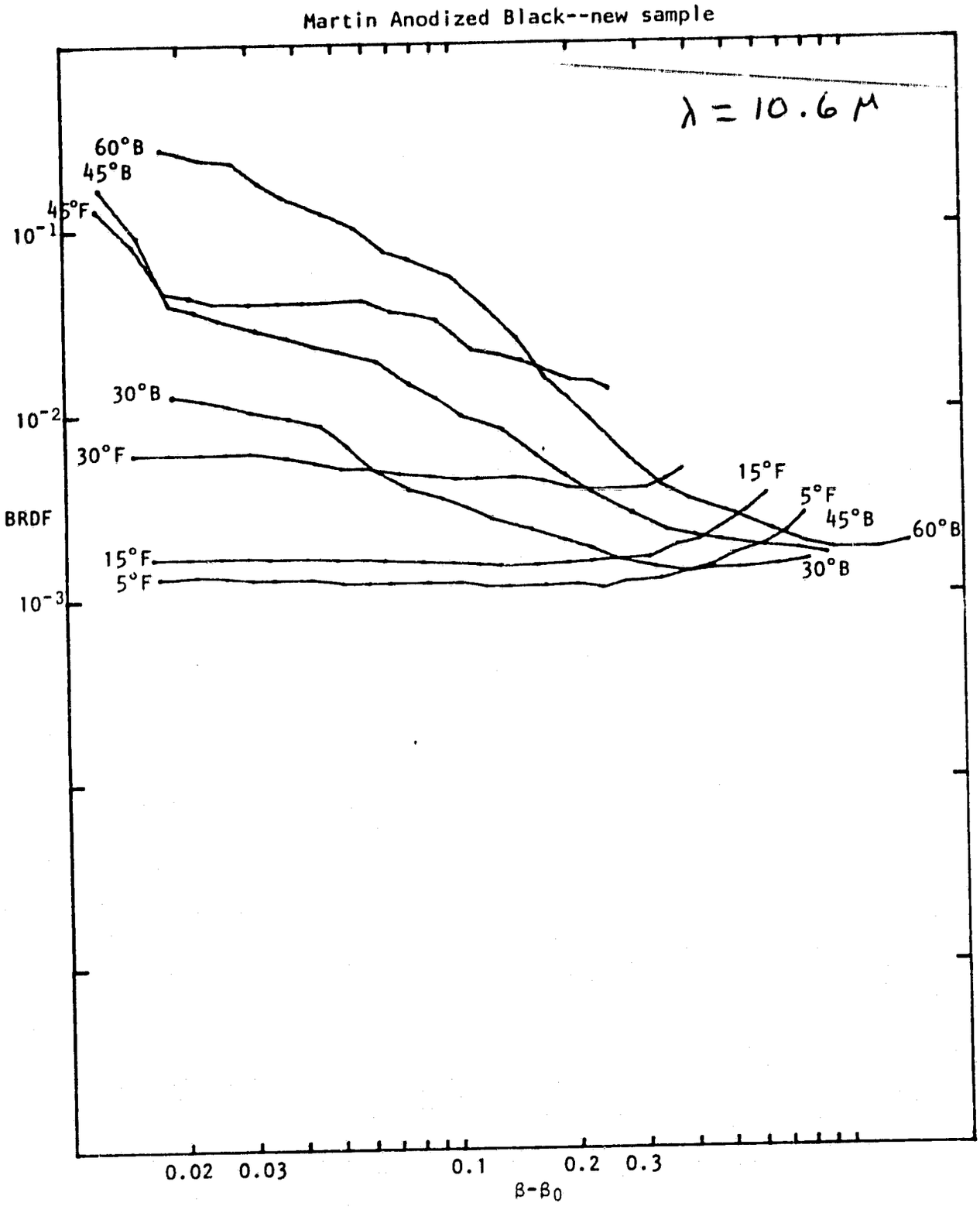
Martin Anodized Black--new sample
λ = 10.6 μ
60°B
45°B
45°F
10⁻¹
30°B
10⁻²
30°F
15°F
5°F
45°B
60°B
BRDF
15°F
5°F
30°B
10⁻³
0.02
0.03
0.1
0.2
0.3
β-β0

Figure 6

BRDF of Polished Mirror Surfaces

Figure 7 shows the results of tests conducted to see which of two polishing compounds gave the lowest light scattering from the polished mirror. Six 5" diameter Cervit samples were polished the same length of time (8 hrs) until all appeared smooth to visual inspection. Three (A-1,2,3) were polished with Cerium Oxide, the others (C-1,2,3) with milled Barnsite. All were tested for scattering characteristics at 10.6 μm. It is seen that neither polishing compound seems to have a decided advantage over the other. Unfortunately, there is no clear explaination as to why some samples tested markedly better than others. (NOTE: Later tests give some indication that most of the differencies may be due to different cleanliness of the samples.)

Figures 8, 9, & 10 show the results of using different coating materials. Each sample (A-1, 2, 3) was cleaned, coated with aluminum in a coating chamber, and tested for scattering properties. They were then stripped, cleaned, recoated with silver, and tested. The process was repeated for a gold coating. Two of the samples (A-1, 3) were also tested "bare" (without a coating). For all the tests a reference sample (#2, Al coated) was also tested to insure that the equipment was working properly.

It is seen that for all three samples aluminum was as good or better (from a low-scattering criteria) as gold, and that silver was consistently poorer. (NOTE: It is believed that silver is not inherently a poorer coating, but that our coating process was, in some undetermined respect, faulty.)

It is interesting that sample A-3, which had the best test results in Fig. 7, seemed superior in these tests; this indicates that A-3 was a somewhat superior substrate.

Figure 11 shows the effects of overcoating a bare aluminum coat with a protective layer of magnesium floride. A sample was cleaned, coated with aluminum (curve 1), stripped, cleaned and recoated (curve 3), stripped, cleaned, coated with aluminum, and overcoated with 1500Å of MgFl (curve 4), and the #4 process repeated except that the overcoat was 750Å (curve 5). Once again, #2 is the "standard".

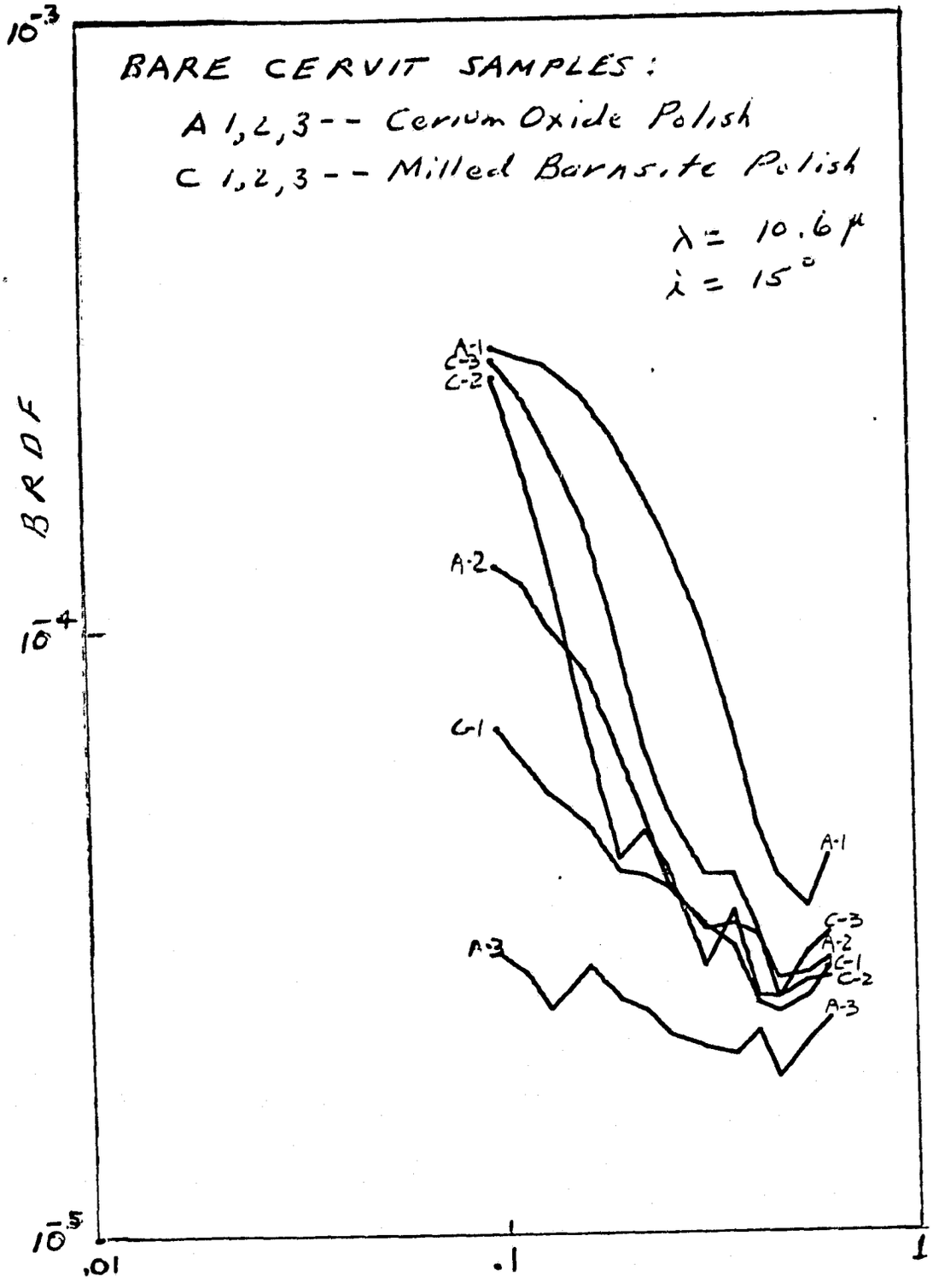
BARE CERVIT SAMPLES:
A 1,2,3 -- Cerium Oxide Polish
C 1,2,3 -- Milled Barnsite Polish
λ = 10.6 μ
i = 15°
BRDF
10^-3
10^-4
10^-5
.01
.1
1
β - β₀
A-1
C-3
C-2
A-2
C-1
A-3

Figure 7

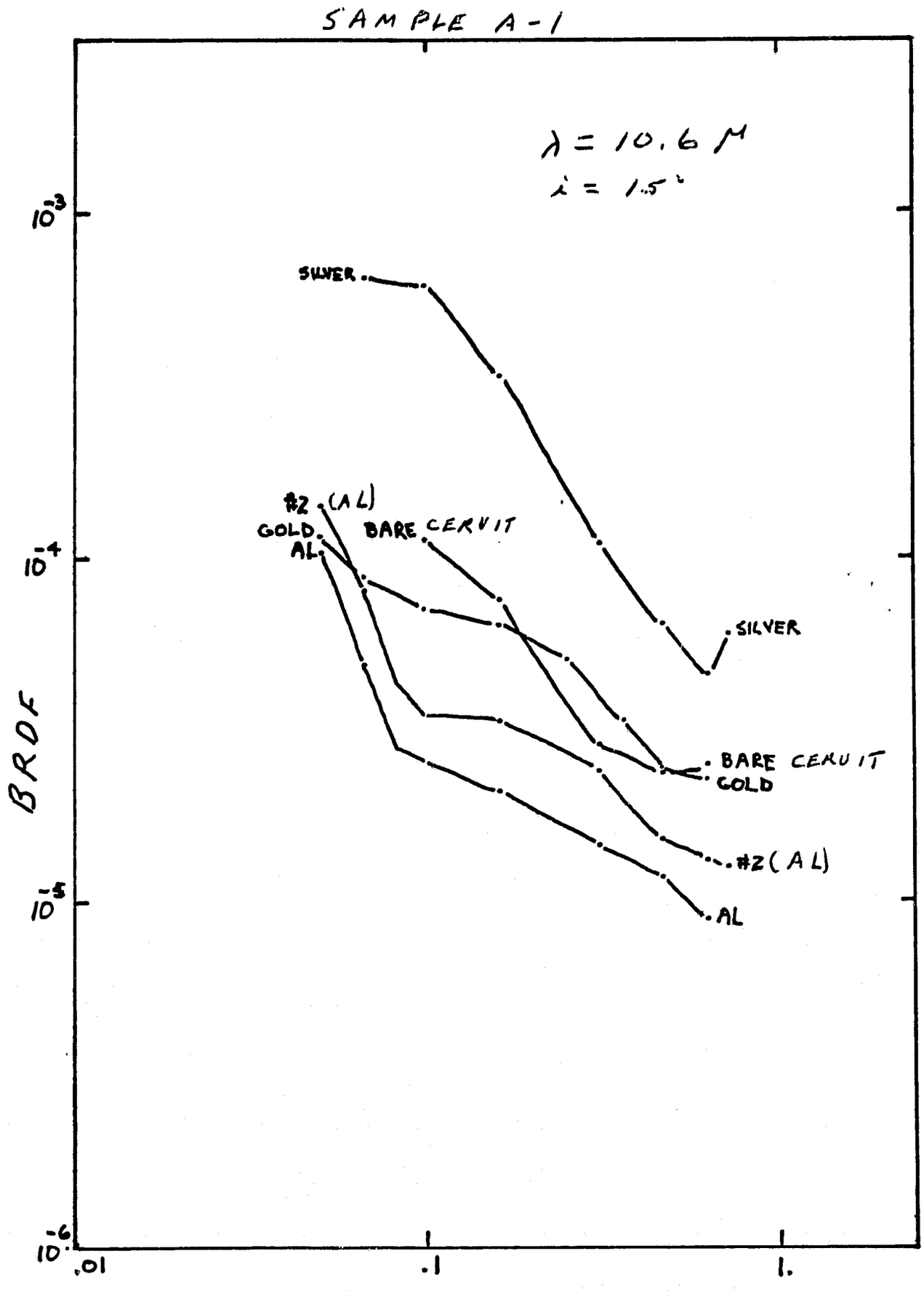

Figure 8

3-21-77

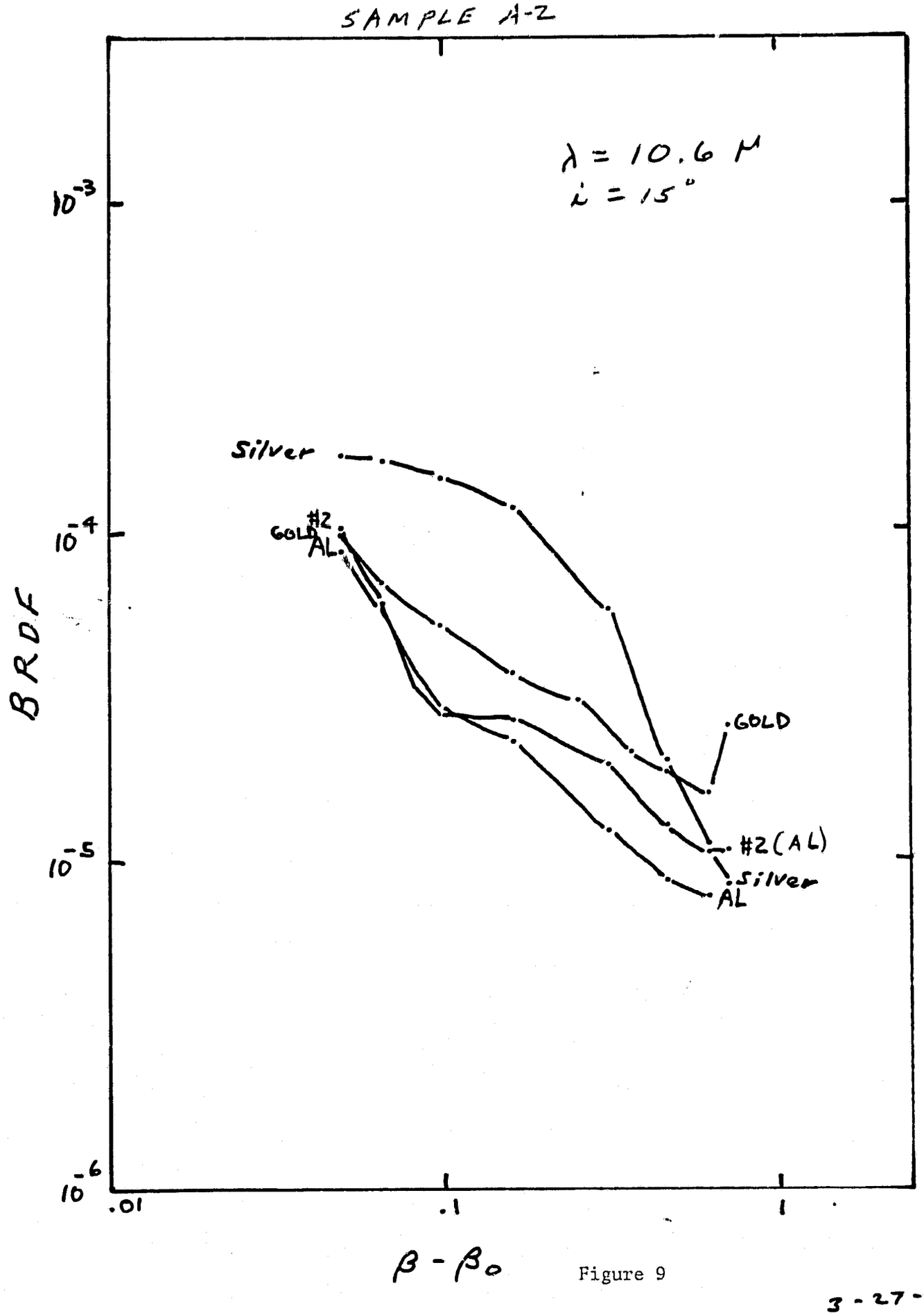

Figure 9

3-27-77

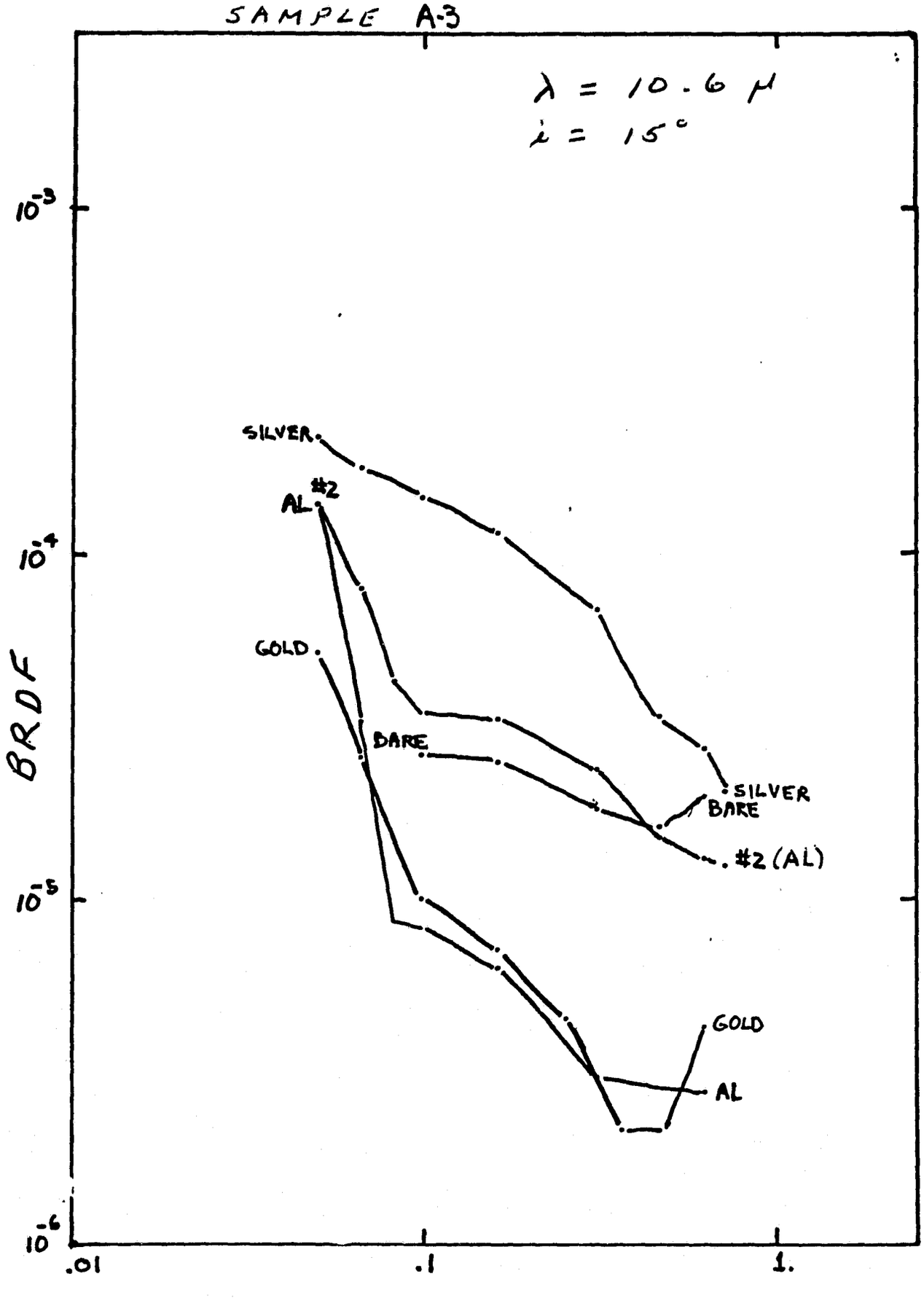

Figure 10

3-21-77

The conclusion is reached that overcoating does not improve the scattering characteristics and may degrade them. (NOTE: It is believed that the 1500Å overcoat was applied too rapidly, so that the overcoat was somewhat rough.)

It was found that scattering tests on bare cervit blanks are meaningful in that they indicate the degree of surface smoothness. However, the reflectivity is so low from uncoated cervit that the signal levels are reduced to such an extent that accurate test are difficult. Figure 12 shows the results of a test to determine if a "spray silver" coat (which can be rapidly applied in a non-vacuum condition) can be used to facilitate scattering tests during a polishing sequence. The results of this test (and of others not shown) reveal that a spray silver coat is too non-uniform to permit its use for tests to determine surface smoothness. (It is commonly used, however, to enhance other optical tests, such as figure sensing.)

Figure 13 shows the results of tests on four different diamond-turned copper mirrors (for use in high-power laser work). The results indicate no decernable trend--the two LASL mirrors have similar shapes but the BRDF decreases with increasing angle faster than a straight line fall-off, which is unusual for mirror surfaces. The Oak Ridge mirror BRDF dropped off very fast with increasing angle--perhaps the values for small angles (less than 8^{o}) from specular had instrumentation problems?? The Spawn mirror was the best of the four and had characteristics more nearly "normal" for mirror surfaces. The effect of polarization is quite apparent for the Oak Ridge mirror--none was noted on the LASL mirrors, and the Spawn was not tested.

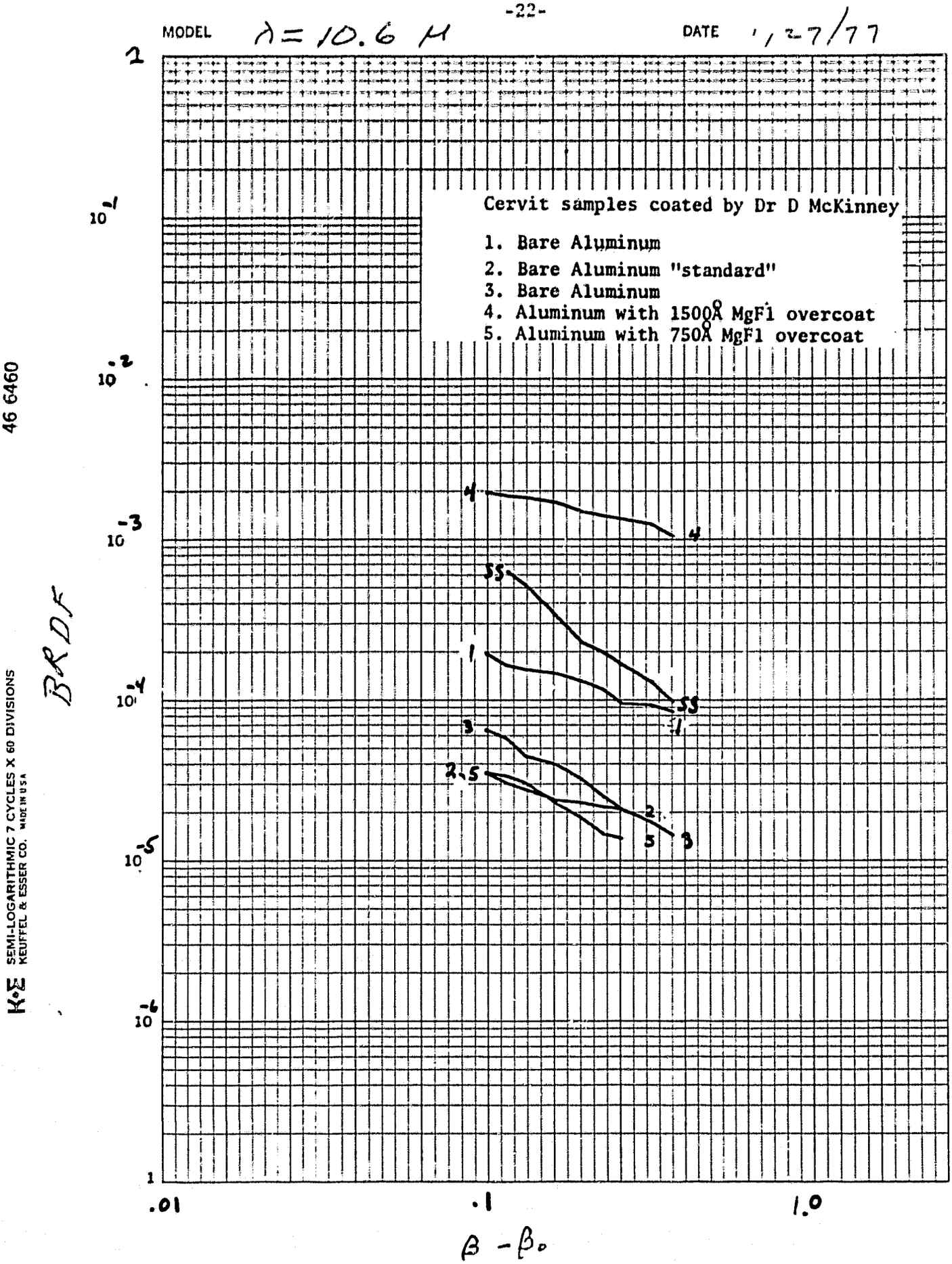
MODEL λ = 10.6 μ
DATE 1/27/77
Cervit samples coated by Dr D McKinney
1. Bare Aluminum
2. Bare Aluminum "standard"
3. Bare Aluminum
4. Aluminum with 1500Å MgF1 overcoat
5. Aluminum with 750Å MgF1 overcoat
BRDF
β - β₀
.01
.1
1.0
46 6460
SEMI-LOGARITHMIC 7 CYCLES X 60 DIVISIONS
KEUFFEL & ESSER CO. MADE IN U.S.A.

Figure 11

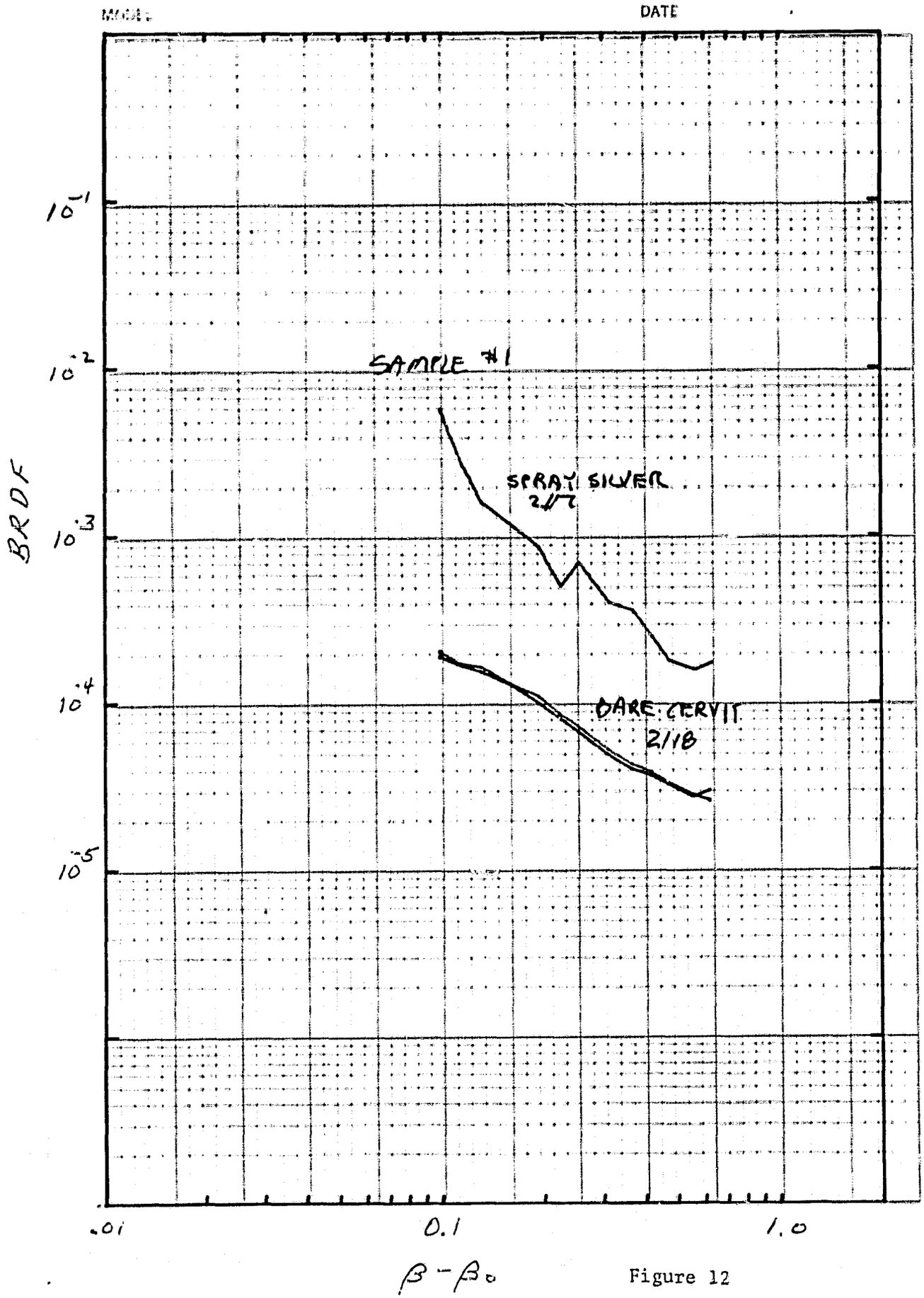

Figure 12

July, 1978 SCATTER FROM S.P.D. DIAMOND TURNED MIRRORS

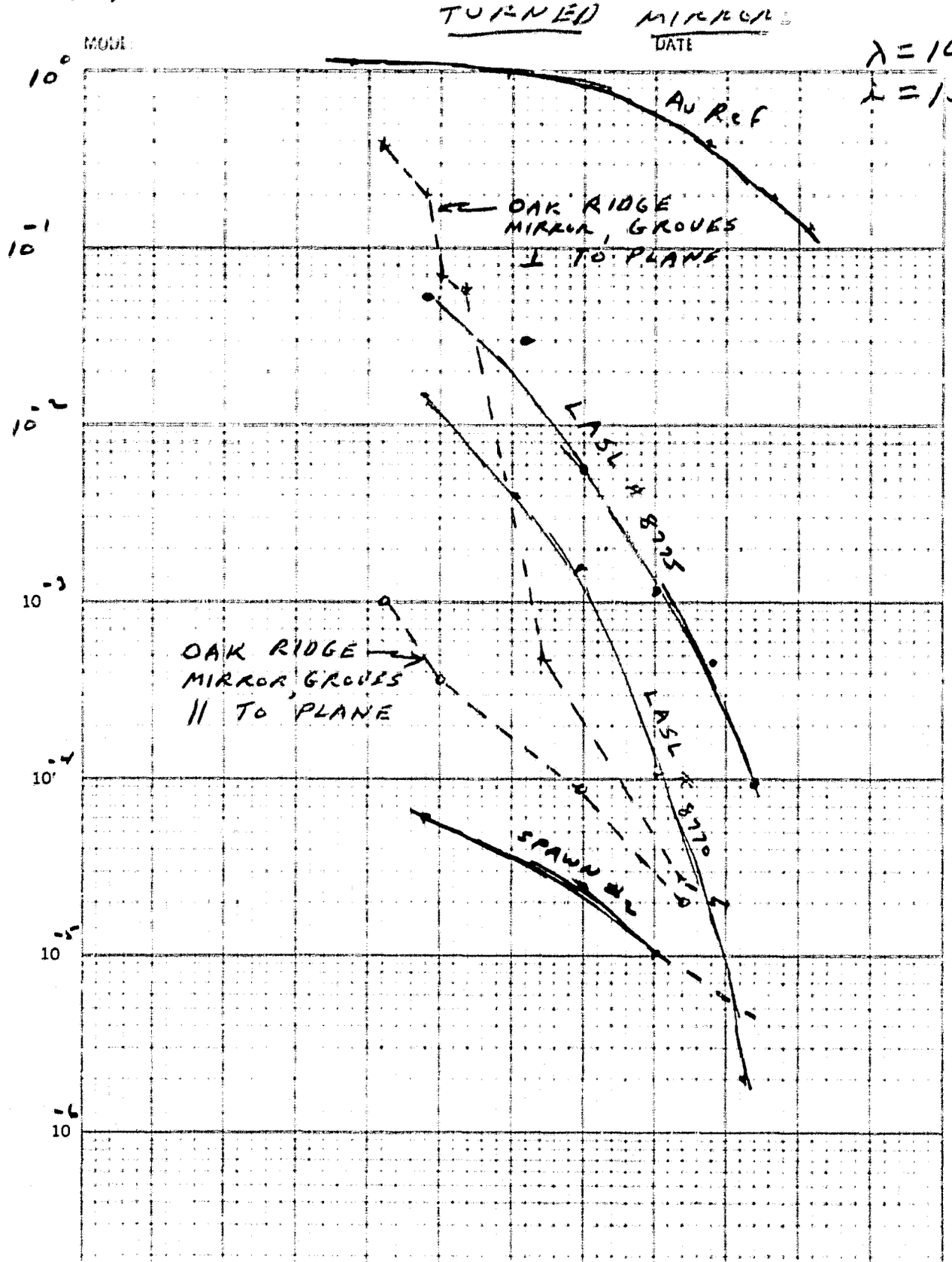

β - β₀

Figure 13

A. Smith & B. Fanning